

NACA RM E57J02

02

1 [REDACTED]
2 [REDACTED] Classification changed to declassified,
effective 1 April 1968 under
authority of NASA OJ [REDACTED]
Change of Security [REDACTED] Carroll. VC

NACA

11 63 13872

RESEARCH MEMORANDUM

PERFORMANCE OF AN INLET HAVING A VARIABLE-ANGLE TWO-DIMENSIONAL COMPRESSION SURFACE AND A FIXED-GEOMETRY SUBSONIC DIFFUSER FOR APPLICATION TO REDUCED ENGINE ROTATIVE SPEEDS: MACH NUMBERS 0.66, 1.5, 1.7, AND 2.0

By John L. Allen

Lewis Flight Propulsion Laboratory
Cleveland, Ohio

LIBRARY
LAWLEY STATION
HAMPDEN VILLAGE

CLASSIFIED DOCUMENT

This material contains information affecting the National Defense of the United States within the meaning of the espionage laws, Title 18, U.S.C., Secs. 793 and 794, the transmission or revelation of which in any manner to an unauthorized person is prohibited by law.

NATIONAL ADVISORY COMMITTEE FOR AERONAUTICS

WASHINGTON
January 30, 1958

UNCLASSIFIED

NATIONAL ADVISORY COMMITTEE FOR AERONAUTICS

RESEARCH MEMORANDUMPERFORMANCE OF AN INLET HAVING A VARIABLE-ANGLE TWO-DIMENSIONAL
COMPRESSION SURFACE AND A FIXED-GEOMETRY SUBSONIC DIFFUSER

FOR APPLICATION TO REDUCED ENGINE ROTATIVE SPEEDS:

MACH NUMBERS 0.66, 1.5, 1.7, AND 2.0

By John L. Allen

SUMMARY

The performance of a two-dimensional side inlet embodying a technique of varying compression-surface angle while retaining a fixed-geometry diffuser was determined at Mach numbers of 0.66, 1.5, 1.7, and 2.0 at zero angle of attack. A 12° compression ramp was faired into the diffuser contour in the conventional manner. However, for larger ramp angles only the ramp forward of the throat bleed slot rotated (leading-edge pivot) and the diffuser contour aft of the slot region remained fixed. The higher ramp angles resulted in step increases in diffuser area in the throat-slot region that were 1.24 and 1.73 times the throat areas for the 17° and 22° ramp angles, respectively.

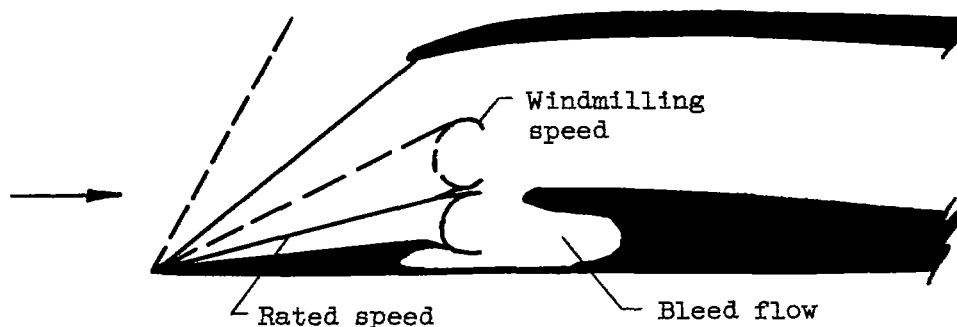
The mass flow captured by the inlet was decreased sufficiently by shock spillage due to increasing ramp angle to satisfy turbojet engine windmilling airflow requirements with total-pressure flow distortions at the diffuser exit less than those for design ramp angle and maximum engine airflow.

Severe ramp boundary-layer separation occurred at Mach 2.0 and to a lesser extent at Mach 1.7. This separation apparently decreased throat bleed effectiveness. Peak pressure recovery for a ramp angle change from 12° to 22° decreased from 0.865 to 0.74 at a Mach number of 2.0, from 0.965 to 0.925 at Mach 1.7, and only from 0.987 to 0.964 at Mach 1.5.

INTRODUCTION

If a turbojet engine becomes inoperative at supersonic speeds (e.g., by flameout), the airflow required for idle or windmilling rotative speed is about one-half that for maximum or rated speed. Since most efficient

inlets do not have a sufficient stable (buzz free) mass-flow range for this amount of normal shock spillage, other spillage systems must be used. One method is to use a bypass arrangement for air in excess of engine requirements (ref. 1). However, the size of the bypass for 50-percent spillage may be larger than feasible for structural and other reasons. Oblique- or conical-shock spillage can be used, but they present some performance and mechanical problems. For two-dimensional inlets having a throat bleed slot the following arrangement may be advantageous:



In essence only the compression-surface angle is increased (leading-edge pivot point) and the subsonic diffuser remains in a fixed position using the throat slot as a dividing region. The cusp-shaped base of the ramp may help establish a trapped-vortex type of flow suggested in reference 2 and thus promote reattachment of the stagnation streamline and reduce the dumping or pressure loss of the sudden area expansion. Reference 3 reports that vortex flow was found only when combined suction and injection were used. Although the diffuser total-pressure recovery was somewhat less than for a conventional diffuser (depending on the throat Mach number), the exit total-pressure distortion was improved. In the range of the tests of reference 4 the cusp shape was not necessary without bleed; however, small amounts of bleed at the sides of the core did energize a vortex and increase the efficiency of the sudden-expansion section to nearly theoretical. For the purpose suggested herein efficiency is not too important, although good distortion levels are desired.

Depending on the efficiency levels obtained, the same concept could conceivably be applied as a variable-geometry inlet-engine matching technique. A lighter weight inlet would result, since only the ramp would need mechanical actuation and the aft diffuser would not require parallel sides.

The results reported herein were obtained in a 1/6-scale side-inlet model (similar to the previous sketch) in the NACA Lewis 8- by 6-foot supersonic wind tunnel. Ramp angles of 12°, 17°, and 22° were tested at zero angle of attack at flight Mach numbers of 0.66, 1.5, 1.7, and 2.0. The 12° ramp was faired with the diffuser surface in the conventional

manner with a bleed slot in the throat region. The 17° and 22° positions resulted in sudden-expansion regions between the ramp base and fixed-geometry diffuser.

SYMBOLS

A	area
A_c	inlet capture area, 0.283 sq ft
A_3	diffuser-exit area, station 3, 0.196 sq ft
h	boundary-layer splitter height
l	diffuser length
M	Mach number
m	mass-flow rate
m/m_0	mass-flow ratio, $\rho VA/\rho_0 V_0 A_c$
P	total pressure
$\Delta P/P_{av}$	total-pressure distortion parameter, numerical difference between maximum and minimum rake total pressures divided by average total pressure, percent
p	static pressure
q	dynamic pressure, $\frac{\gamma}{2} \rho M^2$
R	radius
V	velocity
w	weight flow, lb/sec
$w\sqrt{\theta}/\delta A$	corrected rate of weight flow per unit area, (lb/sec)/sq ft
γ	ratio of specific heats
δ	ratio of total pressure to NACA standard sea-level static pressure of 2116 lb/sq ft
$\hat{\delta}$	fuselage boundary-layer thickness
η	sudden-expansion efficiency

θ ratio of total temperature to NACA standard sea-level static temperature of 518.7° R, also 1/2 equivalent conical expansion angle of diffuser

ρ mass density of air

Subscripts:

av average

b bleed

f final

i initial

max maximum

min minimum

th throat

0 free stream

2 diffuser inlet $2\frac{1}{4}$ in. aft of lip

3 diffuser exit

4 mass-flow station

MODEL DETAILS AND INSTRUMENTATION

General Description of Model

Photographs of the 1/6-scale model are shown in figure 1, and a schematic drawing is given in figure 2. Only one of the twin two-dimensional compression-surface inlets was incorporated on the model, since a separate duct was to be used for each of the twin engines. An open-nose boundary-layer diverter separated the compression ramp from the fuselage by about $h/\delta = 1.33$. A detailed description of the model is given in reference 5.

In order to simulate a variable-angle ramp pivoting about the leading edge, fixed ramps of 17° and 22° were tested in addition to the ramp with the design angle of 12°. The rear or internal ramp surface aft of the throat bleed slot remained fixed for the various ramp angles, as shown schematically in figure 3. The resulting large step changes in diffuser-area variation are shown in figure 4. The internal contraction varied slightly with ramp angle and exceeded the starting limit at the Mach

numbers tested. The generous corner fillets of the 12° design ramp position were not duplicated for the 17° and 22° positions (fig. 1).

The 12° ramp angle is not the optimum compression angle at Mach 2.0, but was taken as the design angle in order to use an existing model.

The throat slot for the 12° ramp was the same as configuration C₄V of reference 5; however, a rearward facing scoop or vent for bleed flow was used on each side of the ramp (fig. 3). Air entering the bleed-flow chamber beneath the ramp was discharged through the vents as well as through the internal model ducting system. Only the ducted bleed flow was measured. The ratio of minimum bleed-slot area to capture area was 0.11, 0.125, and 0.116 for the 12°, 17°, and 22° ramp angles, respectively. To aid in evaluating the experimental results, the following table is presented:

Ramp angle, deg	A ₂ /A _{th}	l/l _{12°} for over-all 2θ = 1.8°	2θ for l = 12° value, deg	Sudden-expansion efficiency, η
12	1.0	1.0	1.8	----
17	1.24	1.85	3.4	0.89
22	1.73	3.0	5.5	.73

The ratio, l/l_{12° , is the ratio of diffuser length to that for the 12° ramp that would be required if the same over-all diffuser expansion angle, $2\theta = 1.8^\circ$, were desired from the throat to the exit (station 2 to 3). Conversely, if the original diffuser length were retained and the diffuser area were faired from the throat to the exit, the over-all diffuser expansion angle would increase as shown. The theoretical efficiency of the sudden-expansion section was computed from the relation

$$\eta = \frac{P_f - P_i}{q_i \left(1 - \frac{A_1}{A_f}\right)^2} \quad (1)$$

When $P_f - P_i$ is obtained from the change in momentum between A_1 and A_f and uniform profiles and incompressible flow are assumed at the two stations:

$$\eta = \frac{2}{1 + \frac{A_f}{A_1}} \quad (2)$$

Equation (1) can also be expressed in terms of total-pressure loss:

$$\eta = \frac{P_f - P_i}{q_i \left(1 - \frac{A_i}{A_f}\right)^2} + 1 \quad (3)$$

Instrumentation

The diffuser exit, station 3, was selected as the compressor-inlet station rather than station 4, which was used in reference 5, since the long duct would tend to reduce the total-pressure distortion and camouflage the effect of sudden expansion. Consequently, a 25-tube area-weighted total-pressure rake was installed at station 3. Six additional total-pressure tubes near the duct wall at a radius ratio of 0.985 were used as a limit for computing total-pressure distortion. The diffuser-inlet total-pressure survey rake shown in figure 3 was present during the entire test and the station 4 rake was used only for computing mass-flow ratio.

RESULTS AND DISCUSSION

Inlet Flow Field

As discussed in reference 5, the local Mach number and total pressure ahead of the inlet were very nearly equal to free-stream values. The local flow angularity at zero angle of attack was nearly aligned with the horizontal axis, or downward $8\frac{1}{2}^\circ$ relative to the inlet centerline, as a result of the $7\frac{1}{4}^\circ$ inlet cant.

Application to Reduced Engine Speeds

Since most turbojets require afterburning in order to provide sufficient thrust for supersonic flight, engine rotative speed is not generally varied to modulate thrust. However, in an emergency such as flameout, damage, or failure, the engine rotative speed will revert to idle or more likely to windmilling speed and the airflow to about one-half the rated value. The main concern is avoiding regions of inlet buzz or instability and high values of total-pressure distortion that could force the compressor into surge and destruction.

Application to a fixed inlet using a bypass for matching rated engine airflow. - Turbojet-engine airflow schedules for maximum or rated, idle, and windmilling rotative speeds at a 35,000-foot altitude are shown in

figure 5. An assumed bypass schedule that efficiently matches the inlet and the maximum-engine-airflow characteristics is shown in order to illustrate application of the data to a fixed-ramp inlet. Of several possible choices, the bypass control was assumed to be scheduled only with flight Mach number, altitude, and temperature. Thus, whenever engine speed is reduced, such as at flameout, the bypass area or position remains fixed in the maximum-speed position and only varies as airplane speed changes.

The basic inlet performance for the various Mach numbers and ramp angles is presented in figure 6. Briefly, increasing the ramp angle from 12° to 22° decreased the mass-flow ratio by means of shock spillage as intended; the level of pressure recovery decreased appreciably at a Mach number of 2.0 and slightly at Mach 1.5. However, at idle or windmilling conditions pressure recovery is unimportant. These results will be discussed more fully later.

Inasmuch as the model used for this investigation was originally designed with a fixed 12° ramp angle, modification to a more optimum ramp angle, say 17° , for a Mach number of 2.0 without a diffuser-area discontinuity was not feasible. Therefore, the 12° -ramp-angle inlet in conjunction with the bypass schedule is taken as a suitable matching combination for the maximum- or rated-rotative-speed airflows, and the ramp angle is assumed to vary only for reduced rotative speeds.

Corrected-weight-flow requirements for maximum, idle, and windmilling engine speeds in conjunction with a bypass schedule are superimposed on the data of figure 6. At Mach 2.0 the stable range of mass-flow ratio for either the design 12° ramp or the 17° ramp is not sufficient to satisfy idle or windmilling requirements. These requirements are satisfied in a stable-flow region by the 22° ramp at a total-pressure distortion slightly less than for the rated-speed condition. Similar results are indicated at other flight Mach numbers. Although only fixed-angle ramps were tested, ramp angle could be scheduled with engine speed so that matching for idle or windmilling conditions would occur at a desired degree of subcritical operation or so that a limiting distortion value would not be exceeded. For inlets without internal contraction, a simple normal-shock sensing control could be used.

A comparison of the total-pressure distortion parameter, $\Delta P/P_{av}$, at station 3 with values for three-dimensional turbulent pipe flow (ref. 6) is shown in figure 7 for a radius ratio of 0.985 (equal to that used at the station 3 rake). The distortion values for each ramp angle for subcritical flow followed the general trend of reduced distortion as corrected weight flow was decreased in accord with reference 6, although the absolute values of distortion differed somewhat. Those for the 22° ramp were higher than pipe-flow values over the range of Mach numbers tested. As discussed previously, the distortion levels at windmilling conditions were somewhat lower than those for rated speed.

The effect of shock spillage on side force was not determined. However, airplane stability, such as yawing moment, could be affected depending on relative spillages of the inlets, inlet orientation, and distance from the center of gravity.

Application to a variable-angle-ramp inlet. - If a variable-angle ramp is used so that efficient thrust-minus-drag performance is obtained over the Mach number range for rated engine conditions, the same principle of increasing ramp angle in order to provide buzz-free inlet operation for reduced rotative speeds could be applied.

If, for example, efficient matching occurred for a ramp angle of 17° at a Mach number of 2.0 and 12° at Mach 1.5, the ramp-angle increases for reduced engine speed would be superimposed on this schedule. The conventional method would be to vary the internal portion of the ramp within the diffuser as the compression-surface angle changes and thus retain a faired diffuser surface and reduced losses for the efficient matching portion. However, the results presented herein indicate that the faired diffuser surface is not necessary for the reduced-engine-speed situation. Thus, only the front part of the ramp needs to be variable for ramp angles greater than those for efficient matching. Obviously, a much simplified design results if the entire range of ramp-angle variation can be accomplished with the rear portion of the ramp within the diffuser remaining in a fixed position. In this case pressure-recovery losses associated with the sudden-expansion section in the diffuser are important.

Inlet Performance with a Sudden Expansion in the Diffuser

Peak total-pressure recovery and maximum mass-flow ratio. - At a flight Mach number of 2.0, peak pressure recovery decreased rapidly from 0.865 for the 12° ramp to 0.74 for the 22° ramp (fig. 6(a)). About 0.03 P_0 of this reduction is attributable to the decrease in shock recovery for the 22° ramp. The total pressure-recovery decrease as ramp angle varied from 12° to 22° was less severe at lower flight Mach numbers: 0.965 to 0.925 at a Mach number of 1.7 and 0.987 to 0.964 at Mach 1.5 (figs. 6(b) and (c)). At Mach 2.0 an indication of the diffuser loss can be approximated by comparing the theoretical oblique-plus-normal-shock pressure recovery with the peak recovery. This loss increased from 0.02 P_0 for the 12° ramp to 0.115 P_0 for the 22° ramp. Shock detachment precludes such comparison at lower Mach numbers. The magnitude of the total-pressure loss due to the sudden expansion as computed from incompressible-flow relations is shown in figure 6(a) to vary from about 0.01 P_0 for the 17° ramp to 0.05 P_0 for the 22° ramp.

The reduction of supercritical mass-flow ratio with increasing ramp angle was primarily due to oblique-shock spillage. The minimum or

4554

supercritical bow-shock spillage, also contributed to mass-flow-ratio changes. Inasmuch as the inlet was overcontracted for each ramp position and operated with a choked throat when supercritical, the mass flow through the throat depended on the average total pressure and area, which were not unique functions of ramp angle because of secondary effects such as separation. A stable subcritical range of mass-flow ratio existed for each Mach number and ramp angle investigated. For some cases the stable range decreased slightly with increasing ramp angle.

CHI-2

The small loss in peak total-pressure recovery at a Mach number of 1.5 was obtained with the same sudden-expansion area ratio and the same order of throat Mach number as that tested at Mach 2.0. However, at Mach 2.0 (and to a lesser extent at Mach 1.7) separation of the ramp boundary layer increased progressively as mass-flow ratio decreased. This separation is shown qualitatively by the schlieren photographs of figure 8. The presence of this separated (low-energy) flow probably reduced the effect of bleed flow and thus retained a high dumping loss in the sudden-expansion section. According to pressure-rise criteria for shock-induced separation, such as presented in reference 7, the normal shock for a ramp angle of 22° at a Mach number of 2.0 would not generally cause separation. It is not known whether the observed separation is due to external effects or to the pressure rise caused by the diffuser-area discontinuity feeding forward.

The losses in the sudden-expansion section were probably large for maximum mass flow, since the throat Mach numbers approached 1 (choked throat) and the bleed mass-flow ratios were relatively small and ineffective. As inlet mass-flow ratio was reduced and the Mach number in the step or sudden-expansion region was decreased, bleed flow increased as bleed-slot pressure increased, and thus, the dumping loss decreased. This trend is reasonably evident at Mach numbers of 1.7 and 1.5 where peak recovery values for the 17° and 22° ramps approach those for the 12° ramp.

The reflexed region of the curve for the 22° ramp at Mach 1.7 was associated with an oscillating bleed-chamber pressure that was not encountered at other conditions. Detachment of the ramp oblique shock seems to thicken the fuselage boundary layer, and this thickening causes a small oblique shock ahead of the ramp leading edge (fig. 8).

Effect of varying bleed flow. - The effects of bleed flow are best shown for a ramp angle of 22° at Mach numbers of 1.5 and 1.7. Figure 9(a) compares the performance over a range of mass-flow ratios both with and without ducted bleed flow (see also fig. 6(d)). The effect of bleed is small until subcritical flow is attained and, hence, the throat Mach number is reduced. Significant increases in total-pressure recovery were obtained with maximum bleed in the subcritical region. The remainder of the data in figure 9 show little effect of bleed flow because the mass-flow

[REDACTED]

ratio m_4/m_0 for which the bleed flow was varied is near the critical-flow region.

Performance at Mach number of 0.66. - The data shown in figure 6(d) at a free-stream Mach number of 0.66 are not in the realm of application but are of interest because of the shock-free external flow. For the range of mass-flow ratios shown, the throat Mach number varies from nearly 1 to about 0.11. Relatively efficient performance, for example, $p_3/p_0 > 0.95$, occurred when the throat Mach number was lower than 0.60, which somewhat correlates with the results of reference 3, which showed good performance at similar diffuser-inlet Mach numbers.

Inlet total-pressure profiles. - As shown by the diffuser-inlet (station 2) total-pressure profiles in figure 10, low-energy flow existed in the step or base of the ramp region and increased in extent as the ramp angle was varied from 12° to 22° . If the rake static-pressure tap is used as a guide, these regions of pressure less than static are separated or exhibit reversed flow. Other instrumentation, such as the claw-type three-directional Pitot-tube rake shown in figure 1(b) in the ramp cusp and bleed-chamber Pitot tubes, did not give any conclusive indication of circulation or vortex-type flow.

Diffuser-exit total-pressure contours. - In addition to the over-all total-pressure distortion at the diffuser exit the distribution of total pressure is also of interest. The diffuser-exit contours (selected contours are shown in fig. 11) indicated no regions of separated flow. Therefore, the separated flow at the diffuser inlet was reattaching before reaching the diffuser exit or perhaps was more like a stationary bubble energized by the throat slot and acting as an aerodynamic diffuser surface.

CONCLUDING REMARKS

The technique of ramp-angle variation with a fixed-geometry subsonic diffuser may possibly have application as an inlet-engine matching device if sufficiently efficient. The data at a Mach number of 1.5 demonstrate that adequate throat bleed results in relatively efficient performance for sudden-expansion area ratios of nearly 2:1. Since the throat Mach numbers for peak pressure recovery were of the same order of magnitude for flight Mach numbers of 1.5 to 2.0 (choked throat supercritically in each case), the large pressure losses at a Mach number of 2.0 are primarily attributed to the effect of ramp boundary-layer separation or low-energy flow on the efficiency of the sudden-expansion section (and to some extent on inadequate bleed). Permitting some initial diffusion prior to the sudden-expansion region by moving the ramp base and slot aft and using an external-compression inlet so that the Mach number in the step region is of the order of 0.60 may reduce the possibility of the sudden-expansion

4554

UNCLASSIFIED

pressure rise influencing ramp boundary-layer separation. If on the other hand the low-energy air is due to external effects, perforation of and bleeding through the ramp would control boundary-layer separation.

SUMMARY OF RESULTS

A side inlet having a two-dimensional compression surface and a throat bleed slot was tested at Mach numbers of 0.66, 1.5, 1.7, and 2.0. The 12° compression ramp was faired into the diffuser contour in the conventional manner. However, for ramp angles of 17° and 22° only the ramp portion forward of the bleed slot rotated and the diffuser contour aft of the slot region remained fixed. The base of the ramp was cusp shaped. The resulting step increases in diffuser area in the region of the throat slot were 1.24 and 1.73 times the respective throat areas for the 17° and 22° ramps. The following results were obtained:

1. The corrected weight flow captured by the inlet was reduced sufficiently by shock spillage as ramp angle increased to satisfy turbojet windmilling airflow requirements. A subcritical stable range of mass-flow ratios was also present over the range of ramp angles and Mach numbers tested and was not significantly reduced by increasing ramp angle.

2. Although large regions of low-energy flow existed in the ramp base region for ramp angles of 17° and 22°, no separated flow was present at the diffuser exit. Flow distortions at the diffuser exit for subcritical flow decreased as duct Mach number was reduced. Distortions at engine windmilling flow for ramp angles greater than 12° were lower than those for the 12° ramp angle at rated engine flow in spite of the area discontinuity that resulted as ramp angle increased.

3. At a Mach number of 2.0, increasing the ramp angle from 12° to 22° decreased peak pressure recovery from 0.865 to 0.74, and the decrease is attributed mostly to severe ramp boundary-layer separation and decreased bleed effectiveness and partly to decreased shock recovery. The corresponding decrease at a Mach number of 1.7, where separation was less severe, was from 0.965 to 0.925 and at Mach 1.5 only from 0.987 to 0.964. Reducing the amount of throat bleed significantly increased these losses in the subcritical region for ramp angles of 17° and 22°.

Lewis Flight Propulsion Laboratory
National Advisory Committee for Aeronautics
Cleveland, Ohio, October 8, 1957

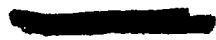
4554

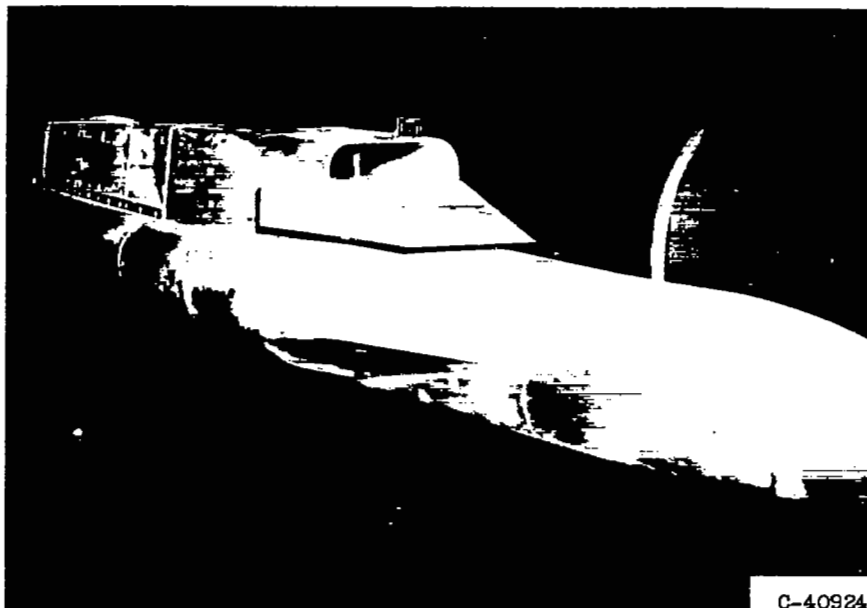
CH-2 back

REFERENCES

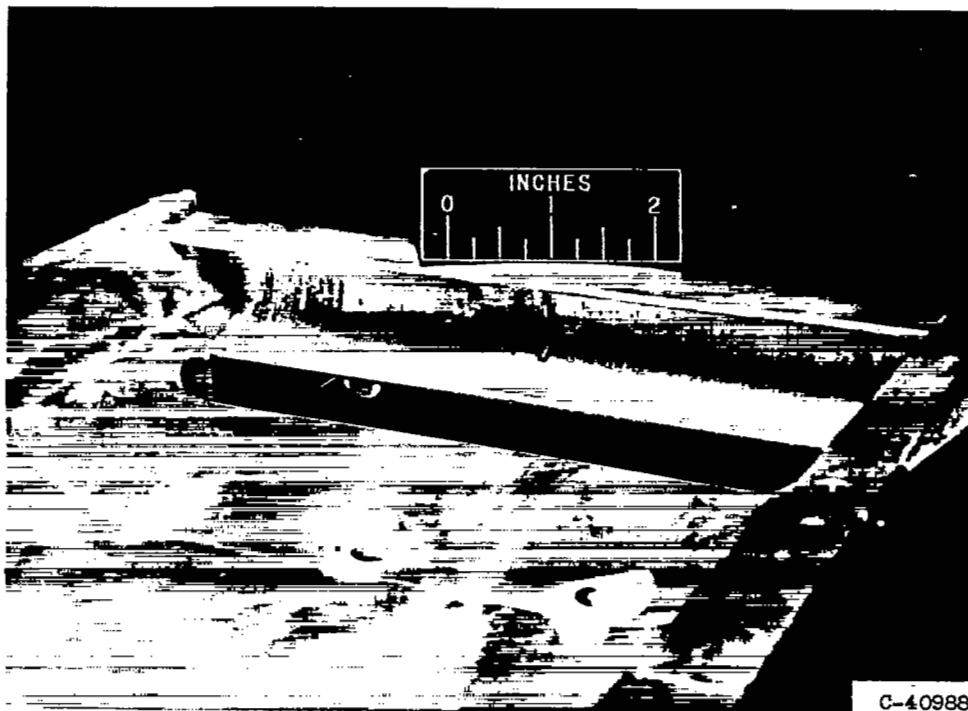
1. Allen, J. L., and Beke, Andrew: Performance Comparison at Supersonic Speeds of Inlets Spilling Excess Flow by Means of Bow Shock, Conical Shock, or Bypass. NACA RM E53H11, 1953.
2. Perkins, Courtland D., and Hazen, David C.: Some Recent Advances in Boundary Layer and Circulation Control. Fourth Anglo-American Aero. Conf. (London), Sept. 15-17, 1953, pp. 189-224; discussion pp. 224A-224N. (Publ. by Roy. Aero. Soc.)
3. Woollett, Richard R.: Preliminary Investigation of Short Two-Dimensional Subsonic Diffusers. NACA RM E56C02, 1956.
4. Hausmann, G. F.: Tests of a Captive-Vortex Diffuser. UAC Res. Dept. Rep. M-13611-1, United Aircraft Co., Sept. 28, 1953.
5. Allen, John L.: Performance of a Blunt-Lip Side Inlet with Ramp Bleed, Bypass, and a Long Constant-Area Duct Ahead of the Engine: Mach Numbers 0.66 and 1.5 to 2.1. NACA RM E56J01, 1956.
6. Sterbentz, William H.: Factors Controlling Air-Inlet Flow Distortions. NACA RM E56A30, 1956.
7. Love, Eugene S.: Pressure Rise Associated with Shock-Induced Boundary-Layer Separation. NACA TN 3601, 1955.

4554



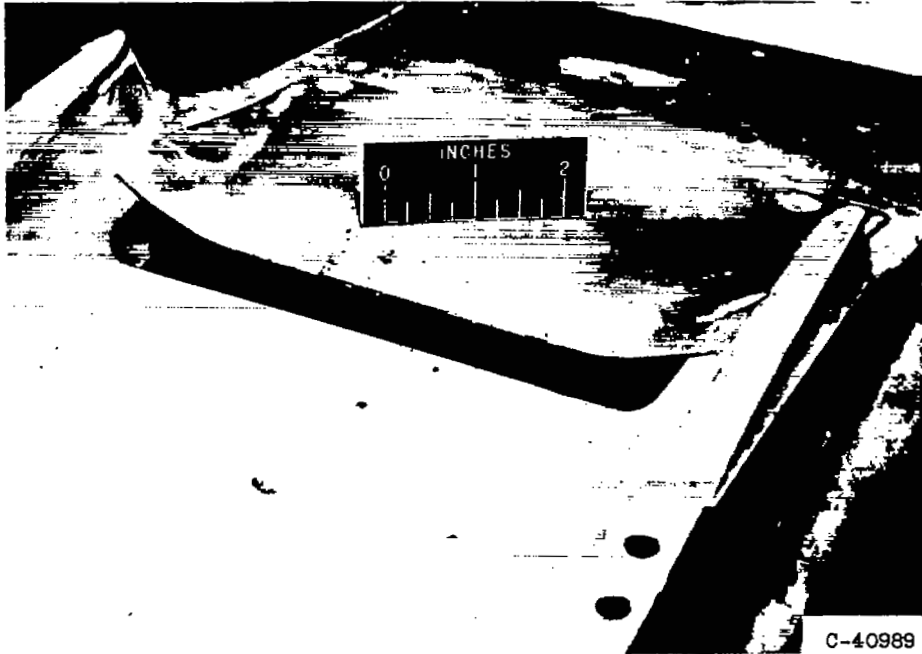


(a) Three-quarter front view. Model rolled 90° ; ramp angle, 22° .

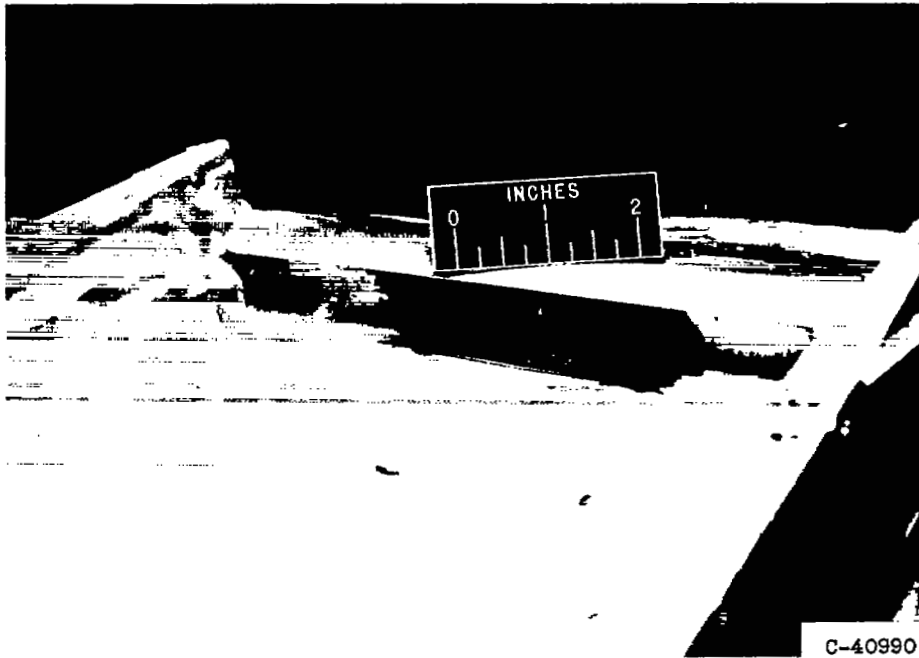


(b) Rear view of inlet throat and ramp. Ramp angle, 22° ; cowl removed.

Figure 1. - Model and ramp photographs.



(c) Rear view of inlet throat and ramp. Ramp angle 12° ; cowl removed.



(d) Rear view of inlet throat and ramp. Ramp angle 17° ; cowl removed.

Figure 1. - Concluded. Model and ramp photographs.

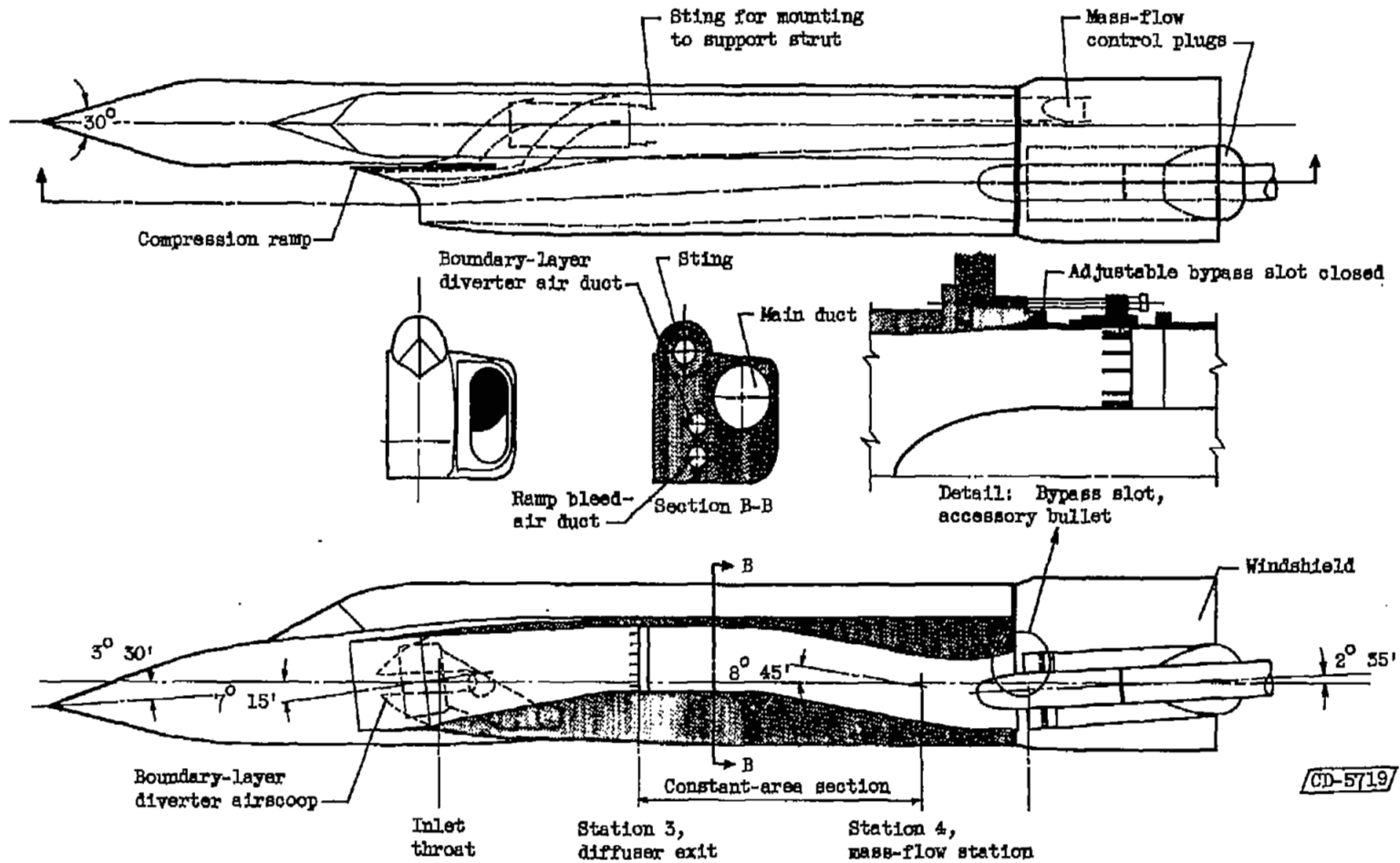
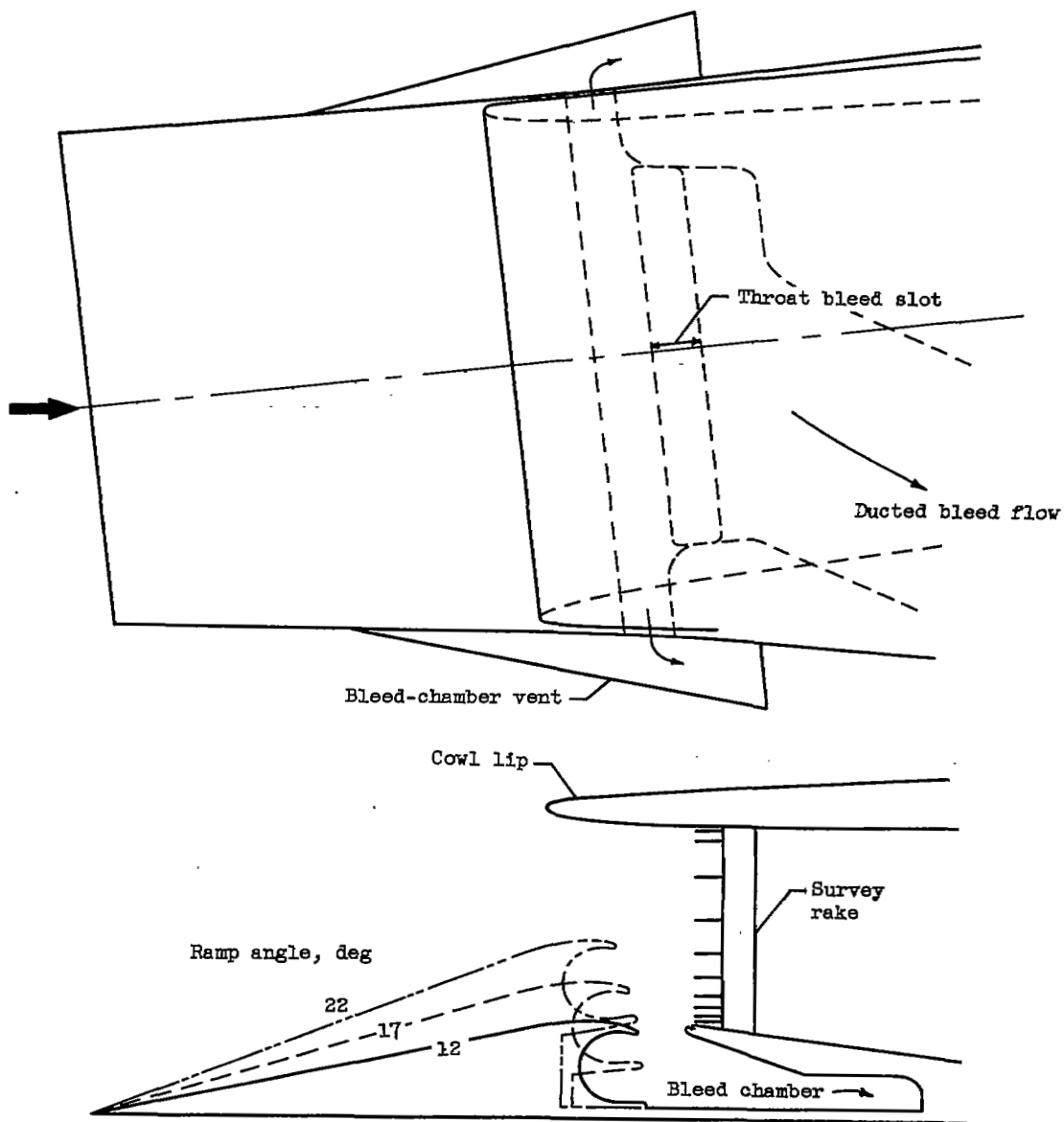


Figure 2. - Schematic sketch of model.





CD-5712

Figure 3. - Schematic sketch of ramp-angle variation and throat-bleed-slot arrangements.

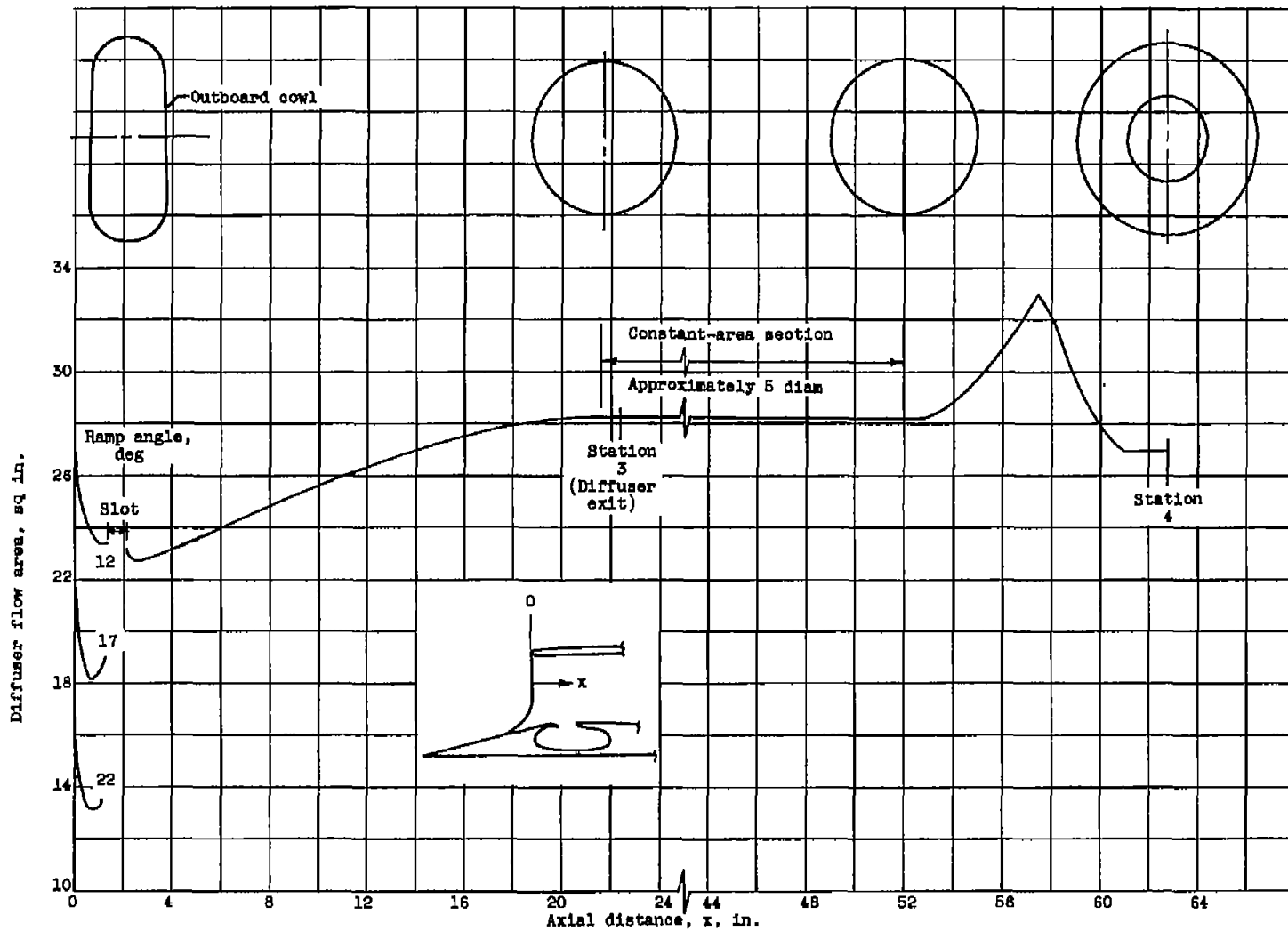


Figure 4. - Diffuser-area variation.

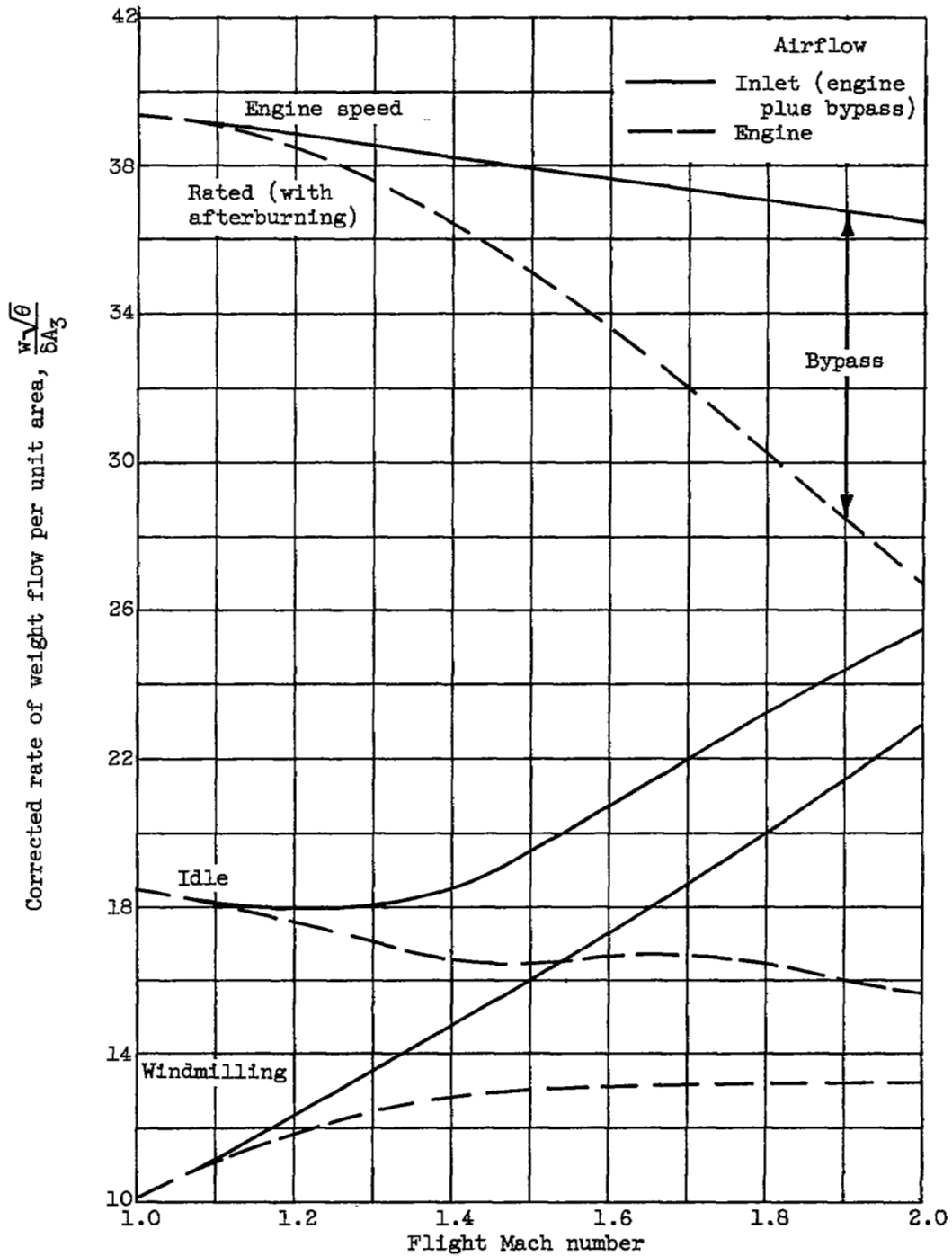
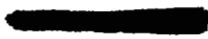
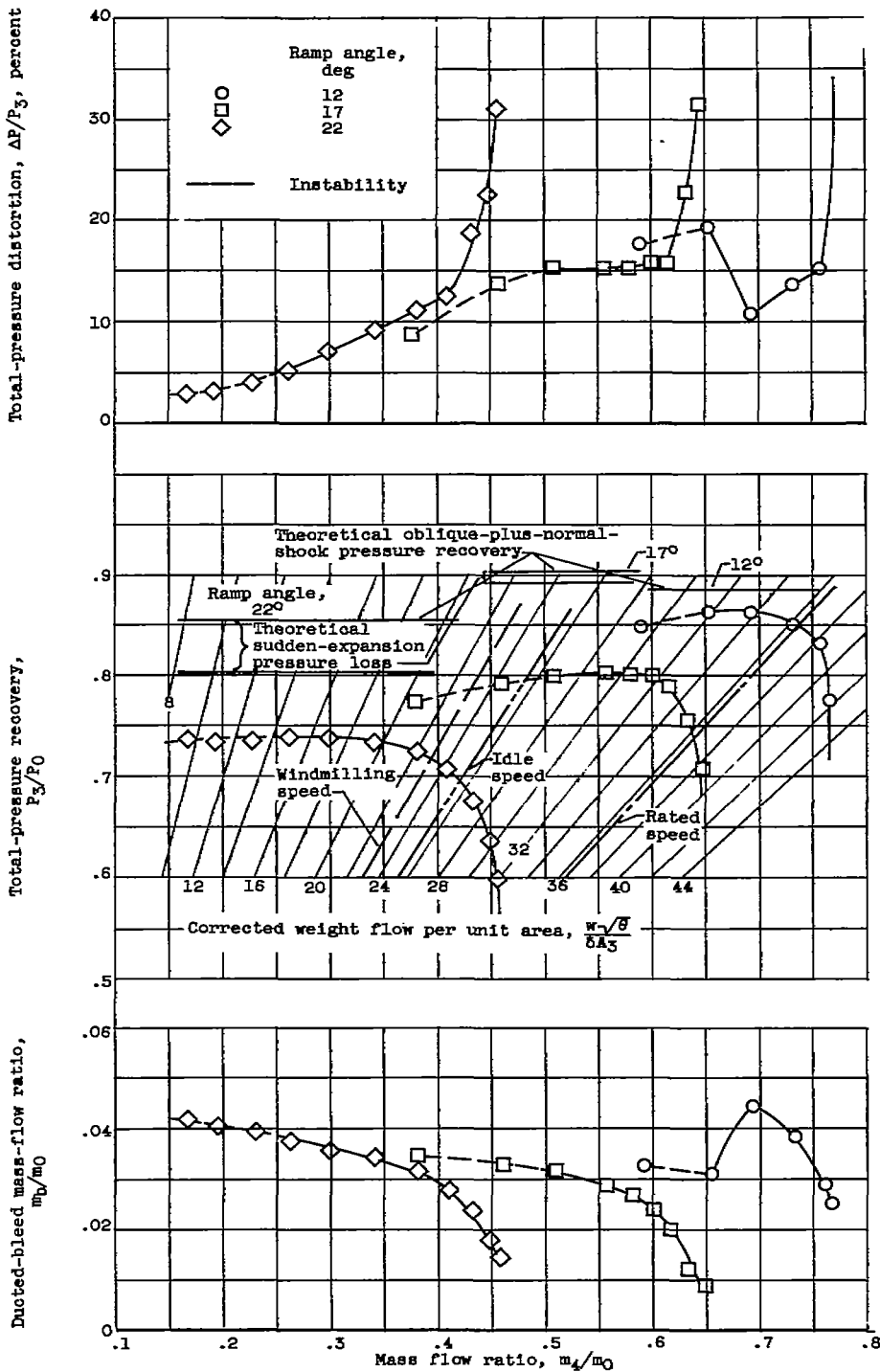


Figure 5. - Engine and bypass airflow schedules.

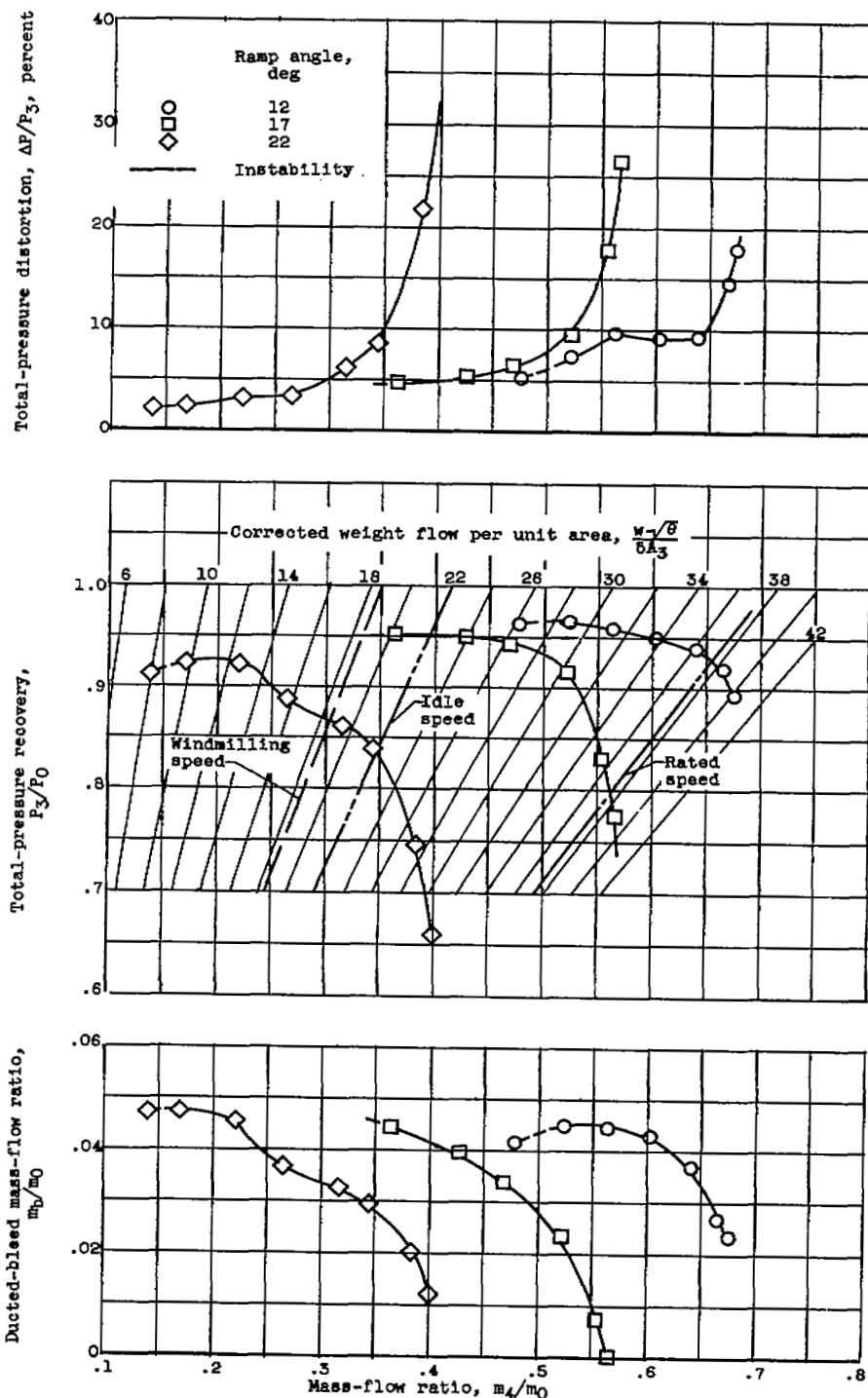


CH-3 back 4554



(a) Flight mach number, 2.0.

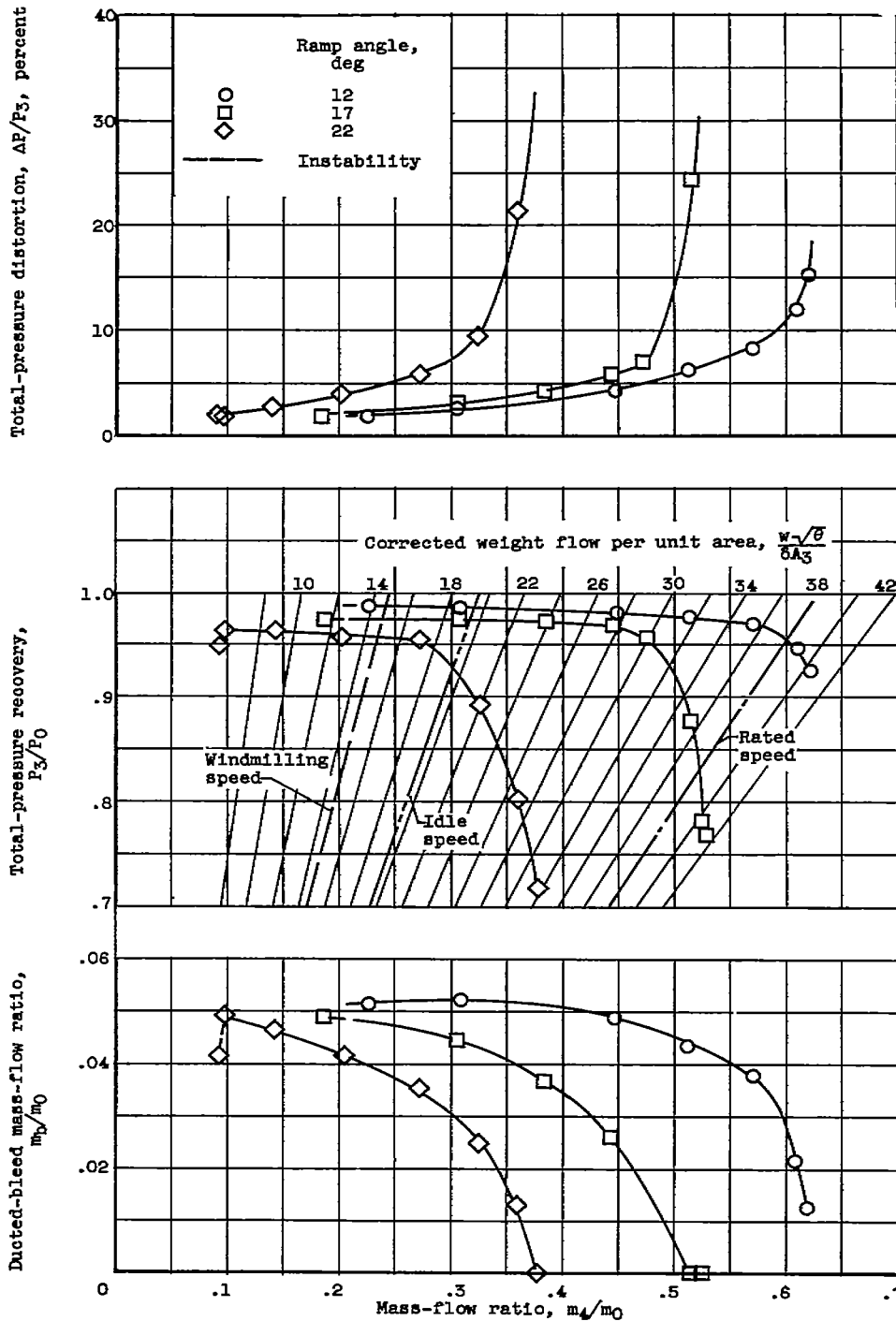
Figure 6. - Inlet performance.



(b) Flight Mach number, 1.7.

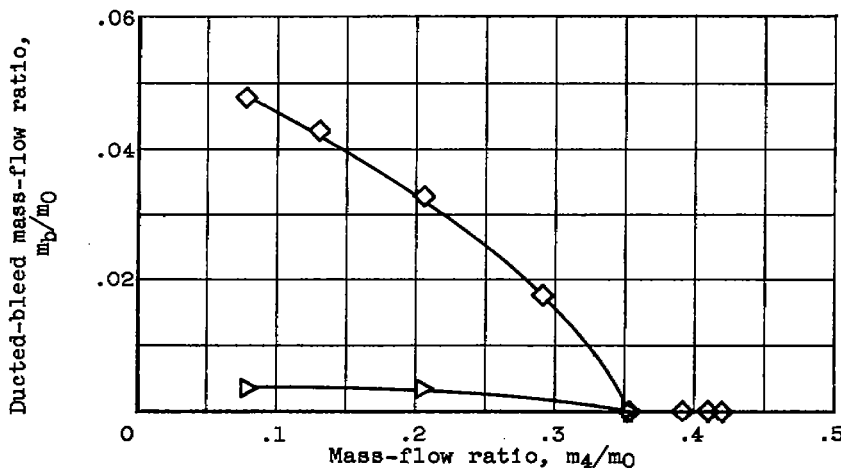
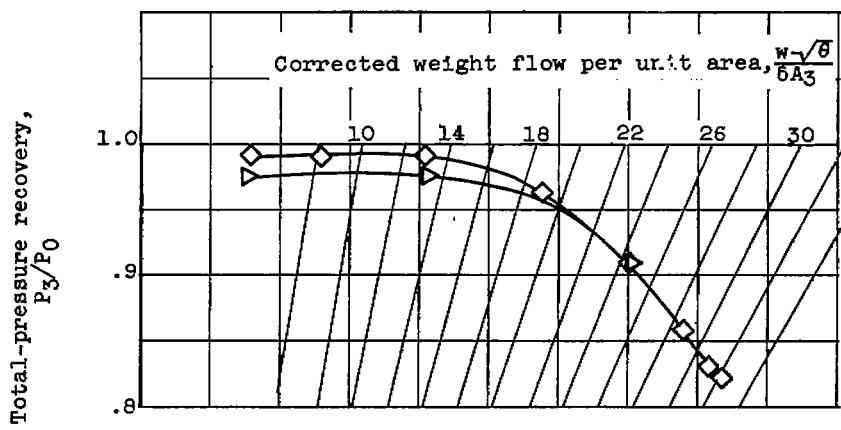
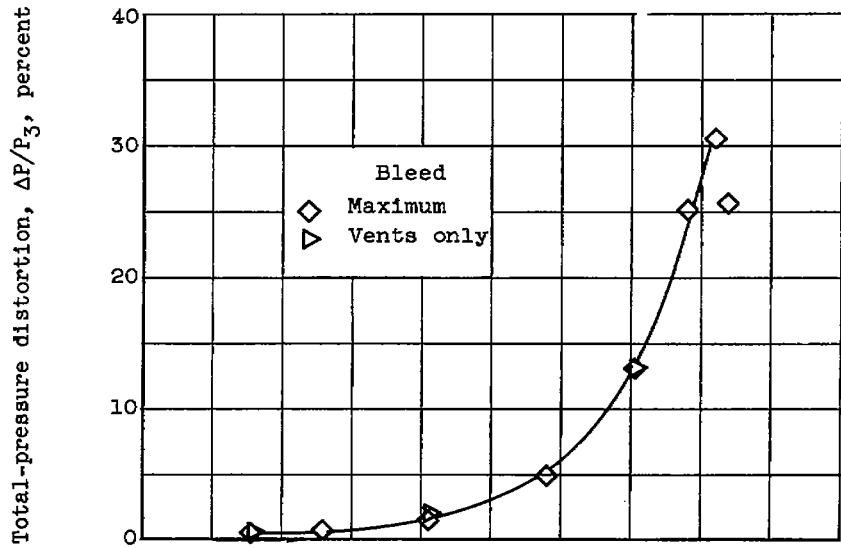
Figure 6. - Continued. Inlet Performance.

4554



(c) Flight Mach number, 1.5.

Figure 6. - Continued. Inlet Performance.



(d) Flight Mach number, 0.66; ramp angle, 22°. Figure 6. - Concluded. Inlet performance.

4554

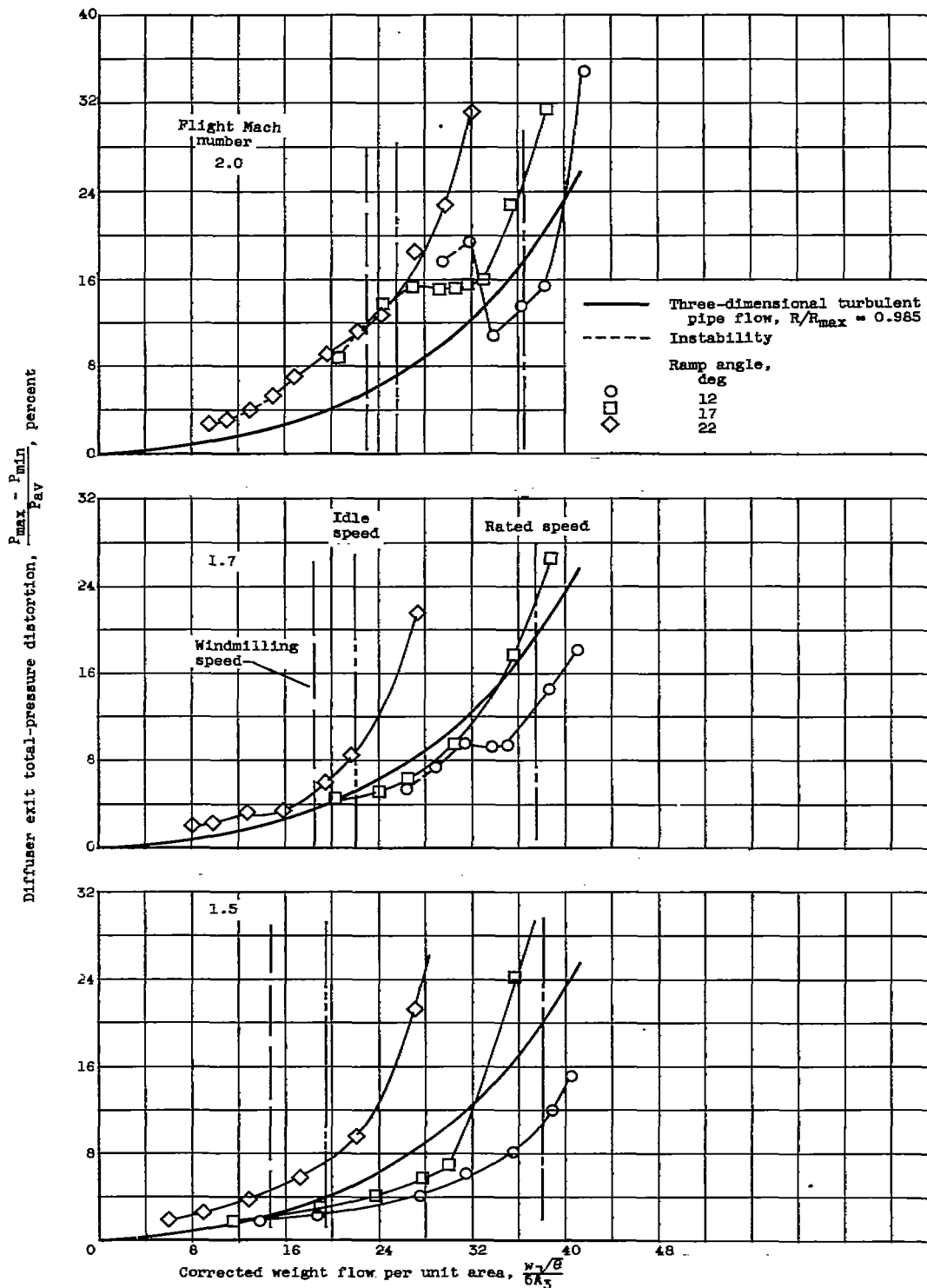


Figure 7. - Comparison of distortions with pipe-flow values.



Ramp angle 12°
Mass-flow ratio, m_4/m_0 0.697



17°
0.509



22°
0.297

(a) Flight Mach number, 2.0.



Ramp angle 12°
Mass-flow ratio, m_4/m_0 0.522



17°
0.427



22°
0.220

(b) Flight Mach number, 1.7.



Ramp angle 12°
Mass-flow ratio, m_4/m_0 0.508



17°
0.306

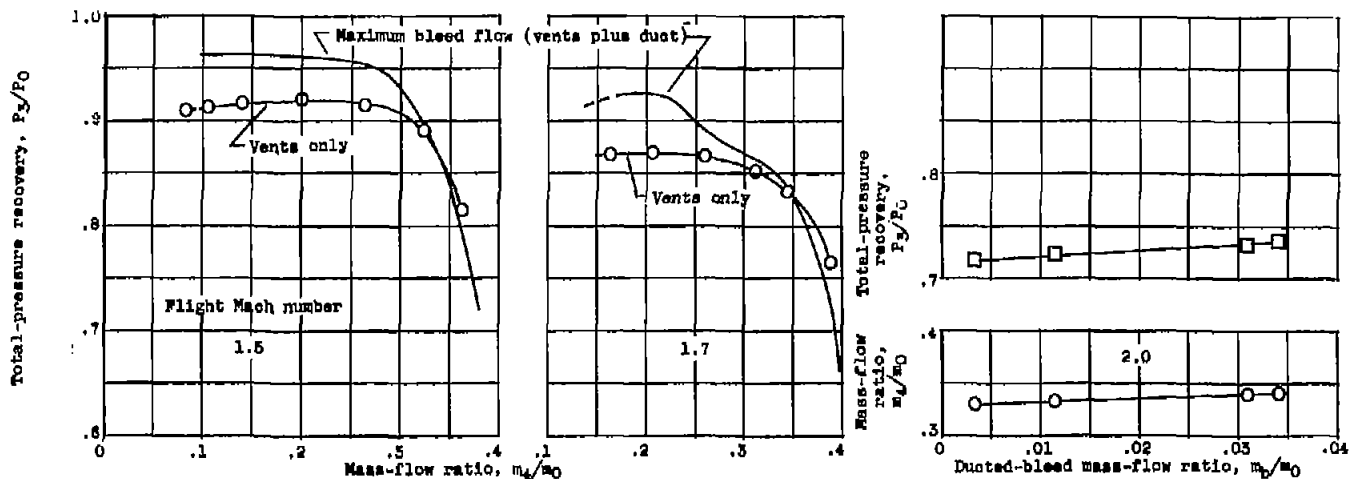


22°
0.203

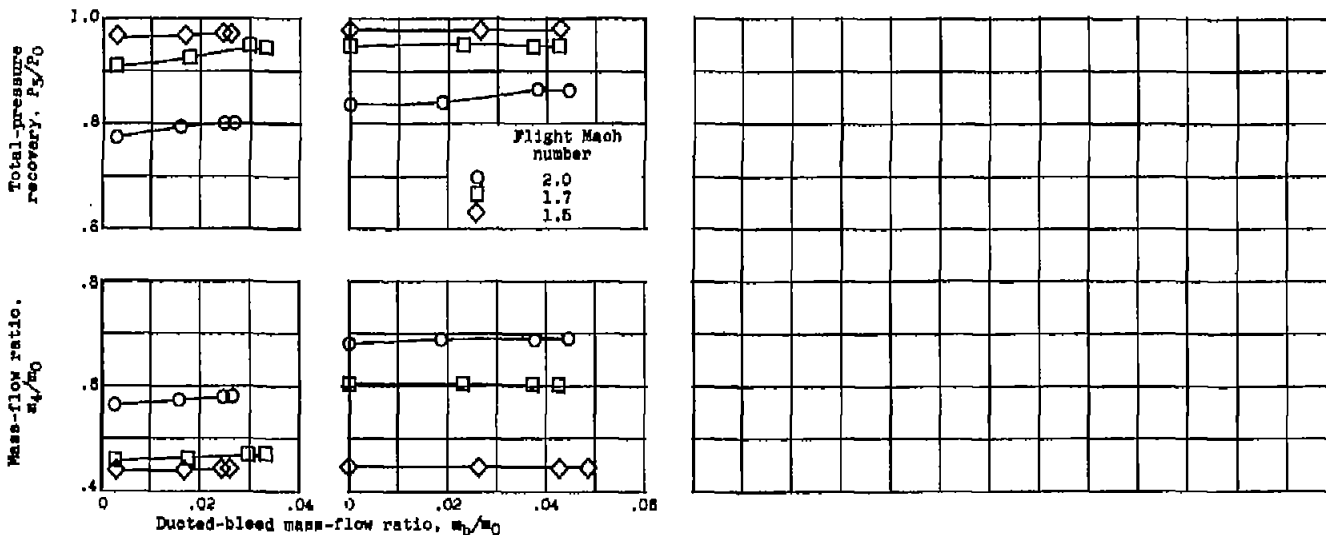
(c) Flight Mach number 1.5.

Figure 8. - Schlieren photographs of inlet.





(a) Ramp angle, 22°.



(b) Ramp angle, 17°.

(c) Ramp angle, 12°.

Figure 9. - Some effects of varying ducted bleed flow.

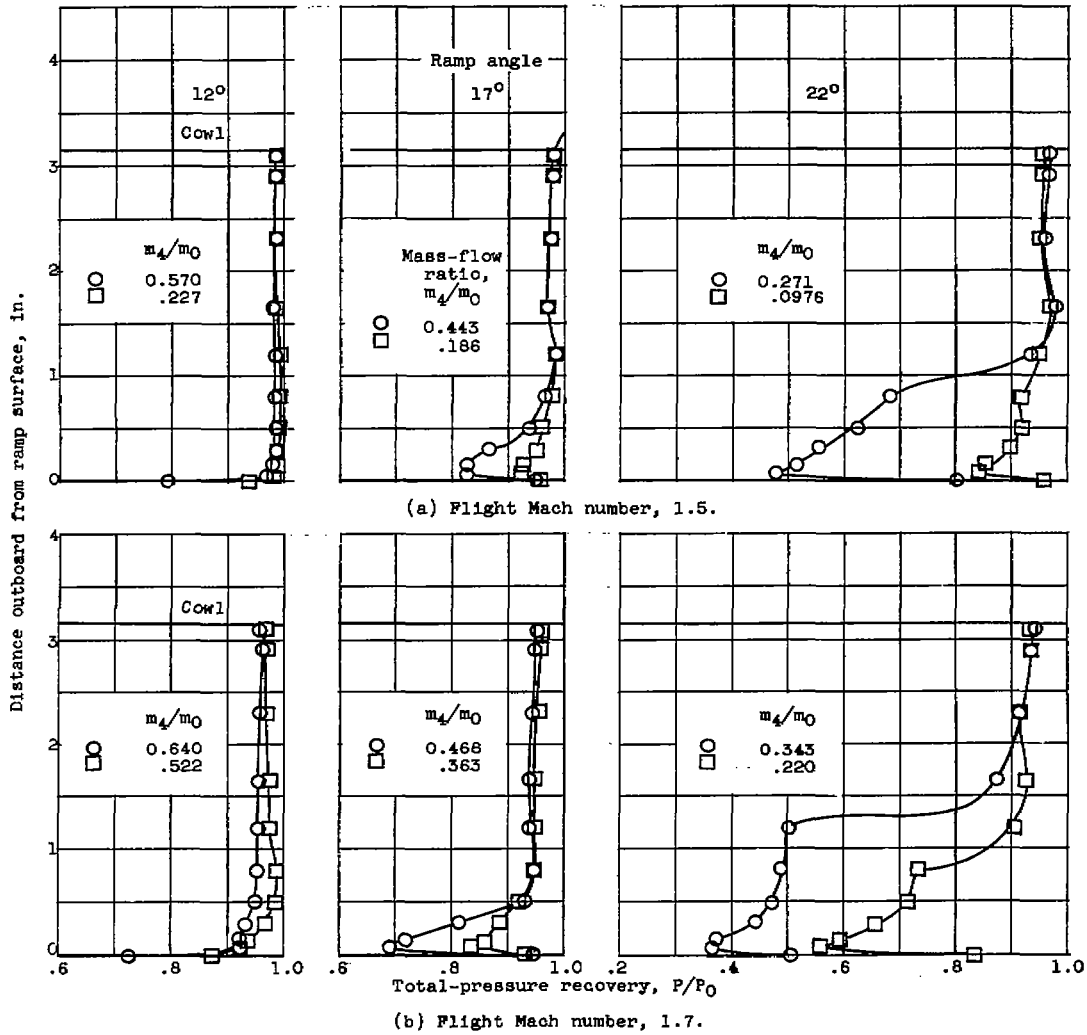


Figure 10. - Diffuser-inlet total-pressure profiles.

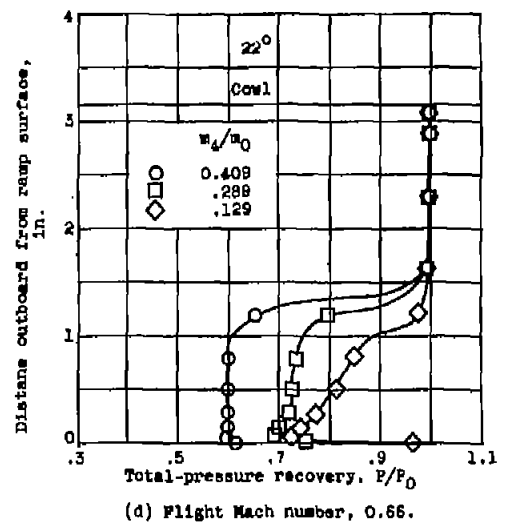
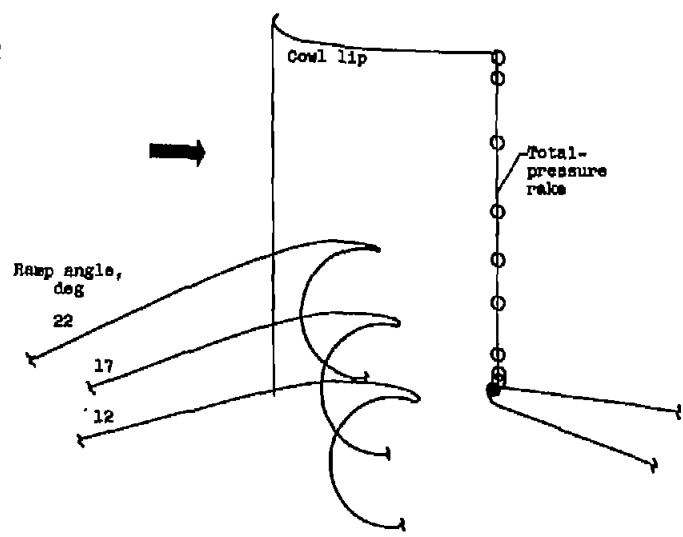
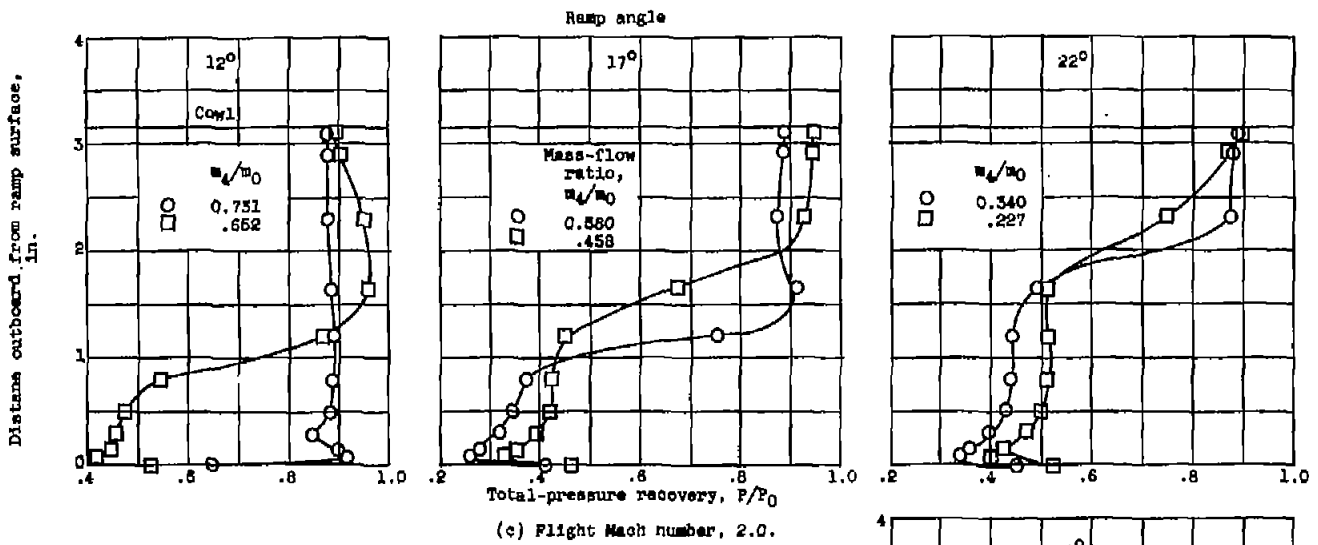


Figure 10. - Concluded. Diffuser-inlet total-pressure profiles.

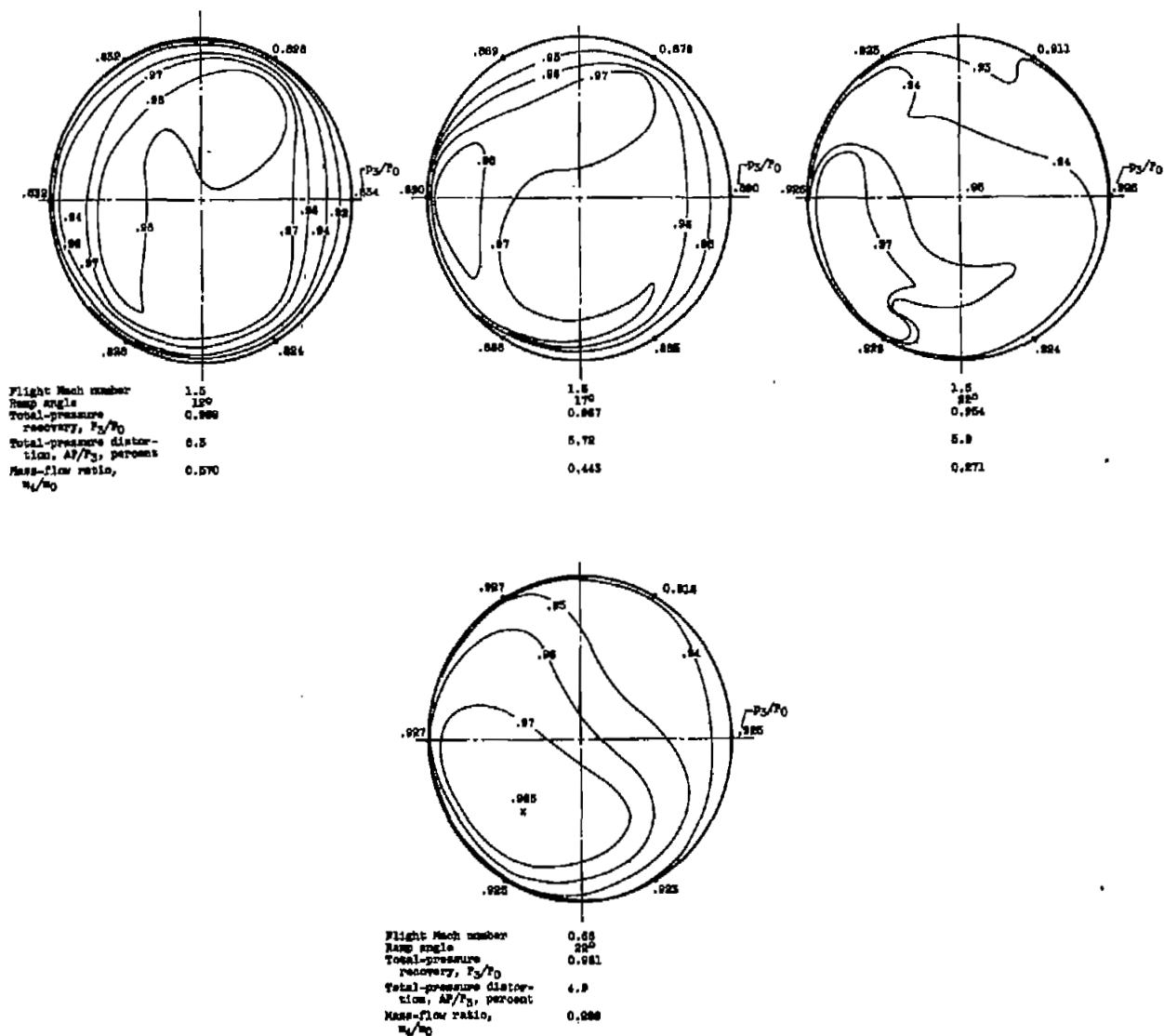


Figure 11. - Concluded. Diffuser-exit (station 3) total-pressure contours. Zero angles of attack and yaw.

NOTES: (1) Reynolds number is based on the diameter of a circle with the same area as that of the capture area of the inlet.

(2) The symbol * denotes the occurrence of buzz.

Report and facility	Description		Test parameters				Test data			Performance		Remarks					
	Configuration	Number of oblique shocks	Type of boundary-layer control	Free-stream Mach number	Reynolds number $\times 10^{-5}$	Angle of attack, deg	Angle of yaw, deg	Drag	Inlet-flow profile	Discharge-flow profile	Flow picture		Maximum total-pressure recovery	Mass-flow ratio			
CONFID. RM ES7302 Lewis 8- by 6-ft super- sonic wind tunnel		1	Throat slot	2.0	1.69	0	0	None	✓	✓	✓	0.865	0.785 to 0.59	12°	Spillage, diffuser-exit pressure distortion, and stability were such that turbojet windmilling conditions were satisfied. Ramp boundary-layer separation at Mach 2.0 decreased performance.		
				1.7	1.65									.965		.680 to .476	Ramp angle
				1.5	1.63									.987		.625 to .225	
				2.0	1.69									.802		.645 to .378	17°
				1.7	1.65									.952		.570 to .362	Ramp angle
				1.5	1.64									.978		.528 to .185	
				2.0	1.62									.740		.456 to .166	22°
				1.7	1.59									.926		.4 to .139	Ramp angle
				1.5	1.58									.963		.378 to .063	
				.68	1.16									.922		.42 to .076	
CONFID. RM ES7302 Lewis 8- by 6-ft super- sonic wind tunnel		1	Throat slot	2.0	1.69	0	0	None	✓	✓	✓	0.865	0.785 to 0.59	12°	Spillage, diffuser-exit pressure distortion, and stability were such that turbojet windmilling conditions were satisfied. Ramp boundary-layer separation at Mach 2.0 decreased performance.		
				1.7	1.65									.965		.680 to .476	Ramp angle
				1.5	1.63									.987		.625 to .225	
				2.0	1.69									.802		.645 to .378	17°
				1.7	1.65									.952		.570 to .362	Ramp angle
				1.5	1.64									.978		.528 to .185	
				2.0	1.62									.740		.456 to .166	22°
				1.7	1.59									.926		.4 to .139	Ramp angle
				1.5	1.58									.963		.378 to .063	
				.68	1.16									.922		.42 to .076	

Bibliography

These strips are provided for the convenience of the reader and can be removed from this report to compile a bibliography of NACA inlet reports. This page is being added only to inlet reports and is on a trial basis.

NOTES: (1) Reynolds number is based on the diameter of a circle with the same area as that of the capture area of the inlet.

(2) The symbol * denotes the occurrence of bumps.

Report and facility	Description			Test parameters				Test data			Performance		Remarks			
	Configuration	Number of oblique shocks	Type of boundary-layer control	Free-stream Mach number	Reynolds number $\times 10^{-6}$	Angle of attack, deg	Angle of yaw, deg	Drag	Inlet-flow profile	Discharge-flow profile	Flow picture	Maximum total-pressure recovery		Mass-flow ratio		
CONFID. RM E57J02 Lewis 8- by 8-ft super- sonic wind tunnel		1	Throat slot	2.0	1.89	0	0	None	✓	✓	✓	0.885	0.765 to 0.59	12°	Spillage, diffuser-exit pressure distortion, and stability were such that turbo-jet windmilling conditions were satisfied. Ramp boundary-layer separation at Mach 2.0 decreased performance.	
				1.7	1.85								.985	.680 to .478		Ramp angle
				1.5	1.83								.987	.625 to .225		
				2.0	1.89								.802	.645 to .378		17°
				1.7	1.85								.952	.570 to .362		Ramp angle
				1.5	1.84								.976	.528 to .185		
				2.0	1.82								.740	.456 to .166		22°
				1.7	1.59								.926	.4 to .159		Ramp angle
				1.5	1.58								.965	.378 to .085		
				.86	1.16								.922	.42 to .076		
CONFID. RM E57J02 Lewis 8- by 8-ft super- sonic wind tunnel		1	Throat slot	2.0	1.89	0	0	None	✓	✓	✓	0.885	0.765 to 0.59	12°	Spillage, diffuser-exit pressure distortion, and stability were such that turbo-jet windmilling conditions were satisfied. Ramp boundary-layer separation at Mach 2.0 decreased performance.	
				1.7	1.85								.985	.680 to .478		Ramp angle
				1.5	1.83								.987	.625 to .225		
				2.0	1.89								.802	.645 to .378		17°
				1.7	1.85								.952	.570 to .362		Ramp angle
				1.5	1.84								.976	.528 to .185		
				2.0	1.82								.740	.456 to .166		22°
				1.7	1.59								.926	.4 to .159		Ramp angle
				1.5	1.58								.965	.378 to .085		
				.86	1.16								.922	.42 to .076		

Bibliography

These strips are provided for the convenience of the reader and can be removed from this report to compile a bibliography of NACA inlet reports. This page is being added only to inlet reports and is on a trial basis.

DATA CENTER



3 1176 01435 8841

DATA CENTER